Journal of Molecular Liquids xxx (2020) xxx

Contents lists available at ScienceDirect

Journal of Molecular Liquids

journal homepage: www.elsevier.com/locate/molliq

Thermodynamic analysis using COSMO-RS studies of reversible ionic liquid 3-aminopropyl triethoxysilane blended with amine activators for CO_2 absorption

Sweta Balchandani [a,b,*], Ramesh Singh [c,*]

[a] Department of Chemical Engineering, Indian Institute of Technology, Guwahati 781039, India
[b] CO_2 Research Group, Department of Chemical Engineering, School of Technology, Pandit Deendayal Petroleum University, Raisan, Gandhinagar 382007, India
[c] Department of Chemical Engineering, University of Pittsburgh at Johnstown, USA

ARTICLE INFO

Article history:
Received 23 September 2020
Received in revised form 8 October 2020
Accepted 3 November 2020
Available online xxxx

Keywords:
CO_2 capture
TESA
COSMO-RS
AEP
APA

ABSTRACT

The non-linearity in the CO_2 absorption process in the novel aqueous blends of TESA and amine activators AEP and APA is studied through COSMO-RS method. The energy associated with each molecule is estimated using Turbomole. Analysis of the chemical compounds for suitable CO_2 absorption is carried out using the trends of sigma potential and sigma surface. Various significant thermodynamic properties (activity coefficient, chemical potential, excess enthalpy and excess Gibbs free energy, infinite dilution activity coefficient) and thermophysical (vapor pressure, density, viscosity) properties of the blends are estimated and compared with the experimental data. The binary interaction parameters for the systems under study using NRTL, WILSON and UNIQUAC 4 models is carried out. All the interaction parameters are functional to temperature and molecular properties of the constituents involved. CO_2 solubility of three blended solvents at various concentration and temperatures is reported at (1.0–3.0) bar solute partial pressure. Important chemical reaction parameter *pKa* of the amine activators in various solvents is estimated at room temperature. An insightful study for the studied systems indicate their possible usage for CO_2 absorption and of the many systems studied, the best suitable solvent being aq. (TESA + APA).

1. Introduction

Contributing 36.81 K Mt. CO_2 in 2019, it is one of major greenhouse gas emitted through various large point sources. Due to the same fact, a great attention in development of newer and better solvents for CO_2 capture have been a key research area over decades. From exploring the base chemistry of the traditional amine solvents [1,2], to further development of new solvents based on ionic liquids [3], amine activators [4], etc. or blended solvents of different categories which provide better properties of thermal stability and high CO_2 capture capacity [5–7]. Although, a lot of work has already been published in similar lines where through experimentation various important properties such as CO_2 solubility, density, viscosity, surface tension, diffusivity, kinetic parameters, etc. have been obtained. Yet, many of the thermodynamic and molecular analysis is still need of the hour due to limitations in application of such solvents because of lack of data. Neuro-fuzzy approaches [8], mathematical regressions and artificial neural network [9], thermodynamic co-relations [10], molecular analysis [11–13], and machine learning and optimization strategies [14,15] are currently being explored for various carbon capture and storage (CCS) engineering applications. The major focus being the same for all the techniques-to have a deep understanding of the system as well as to study the non-ideal system.

Conductor like screening models for real solvents (COSMO-RS) is another category of quantum based model explored in the present study. COSMOtherm-an advanced quantum mechanics software has been earlier studied for variety of applications. An insightful thought on the diverse analysis possible through the COSMO-RS method can be reviewed from various research contributions in the literature [16–19]. The useful remarks of the associated work are presented in the along section. Zhang et al. [20] studied the problem of tar accumulation in biomass gasification and examined various solutes for the dissolution using COSMOtherm. They also gave a brief comparison of the experimental data with the Aspen simulation which yielded a goad agreement. Through COSMOtherm, the main aim by estimation of infinite dilution activity coefficients is search for an optimal solvent giving a fair absorption capacity. It was concluded that

* Corresponding author at: Department of Chemical Engineering, Indian Institute of Technology, Guwahati 781039, India.
E-mail addresses: sweta.balchandani@iitg.ac.in (S. Balchandani), rsingh@pitt.edu (R. Singh).

https://doi.org/10.1016/j.molliq.2020.114713
0167-7322/

absorbents with strong polar groups are appropriate for phenol removal.

Water removal from methanol/ethanol which are usually used as an additive in the fuels has been studied using the ionic liquid [emim] [dca] at (323.15–363.15) K in the concentration range for ionic liquid being in mole fractions of (0–0.5) and reported in the literature [21]. The vapor pressure analysis, vapor liquid equilibria and subsequent sigma profile derivation of the compounds was carried out through COSMO-RS simulation. It was concluded that there is a strong interaction between water and methanol/ethanol in comparison to [emim] [dca] ionic liquid. Partition coefficients being one of the major criteria to acknowledge the separation process involving various solutes and solvents was also analysed for octanol-water system [22] where the deviations from the experimental data was 4.92% indicating a quite efficient prediction. The authors further gave in depth analysis for development of materials from quantum chemistry to mesoscale properties in the material science field. In similar lines, the liquid-liquid equilibrium studies which play an important role for integrated designing of the industrial process were presented where the partition coefficients related to catalyst ligand biphephos were estimated [23].

Excess enthalpies and sigma profile studies for various valuable chemicals and their blends i.e. (glycerol formal +1, 2-propanediol), (glycerol formal + ethylene glycol), glycerol formal+ glycerol), (solketal +1, 2-porpanediol), (solketal + ethylene glycol), and (solketal + glycerol) were presented over a temperature range of (298.15–313.15) K at 1 atm [24]. The volumetric behaviour through excess molar volumes and viscosity deviations were further analysed through first principle Redlich-Kister and Jouyben –Acree models. The experimental and modeled data presented a least deviation of 0.364%. Although, the Jouyben- Acree model was proved to be good for density estimation whereas for viscosity, the highest deviation was found to be 432.11% indicating its lower estimation quality. The screening of 240 ILs as solvents for extraction of petroleum asphaltene through COSMO-RS method is also reported [25]. The authors concluded that aromatic cation [bmim] with anions such as $[NS_2O_4C_2F_6]$, $[C_6F_{18}P]$ and [B (CN) $_4$] yielded better performance for extraction of asphaltene. The studies by the authors was further explored in terms of effect of cations and anions on the removal and σ-profile analysis.

However, similar studies on CCS (carbon capture systems) are less available in the literature. A molecular interaction and simulation study of CO_2 solubility in deep eutectic solvents have been reported [26,27]. It was observed that Allyltriphenyl Phosphonium bromid (ATTPB) Triethylene Glycol (TEG) was found to be promising solvent amongst the five other solvents with also a least deviation between experimental and simulation study. The max CO_2 solubility in (ATTPB TEG) was observed to be $x_{CO2} = 0.527$ at 1.950 MPa. In view of this, sigma profile analysis, estimation of vapor pressure, prediction of pure component viscosity, density, infinite dilution activity coefficients, VLE analysis, estimation of Henry's constant and *pKa* values for aq. 3-aminopropyl triethoxysilane (TESA), aq. 1-(2-aminoethyl) piperazine (AEP) and Bis (3-aminopropyl) amine (APA) and/or various combinations of these solvents have been studied in the present work. The possibility of AEP and APA as good potential solvent activators for CO_2 capture has been earlier discussed in our previous work [7,28,29]. The reversible ionic liquid (IL) nature of 3-aminopropyl triethoxysilane (TESA) is being earlier discussed in the literature [30–32] proving it to be a prospective better solvent. The main advantage of TESA over other amines and ILs is that it exhibits characteristics of both. In the initial level of reaction, it acts as amine due to the presence of amino group, whereas in the latter stage it gets converted into carbamate anion and cation. In comparison to usual ILs such as imidazolium or phosphonium, the comparative costs of TESA is quite low and hence the overall absorption costs down to less. TESA has also shown to be thermally very stable in the previous studies. The present work therefore has major focuses on proving the capability of TESA + AEP/APA to be impending solvents for CO_2 capture through the molecular analysis of the systems through review of several molecular and thermodynamic properties using COSMO-RS

2. Computational methods and theory

The molecules under study i.e. 3-aminopropyl triethoxysilane (TESA), H_2O, CO_2, 1-(2-aminoethyl) piperazine (AEP) and Bis (3-aminopropyl) amine (APA) were selected within COSMOtherm (COSMOlogic GmbH, Leverkusen, Germany). Single conformers with least energy at the ground state were selected for each of the molecular compounds featured with BP-TZVPD-FINE level COSMO calculations which incorporates a full geometry optimization by density functional theory (DFT) using the Becke and Perdew (BP) functional with Triple-Zeta Valence Polarized (TZVP) basic set. Sigma surface and sigma potential estimation, vapor pressure analysis, pure component density and viscosity, infinite dilution activity coefficients, vapor liquid equilibrium analysis, CO_2 solubility, Henry's constant, and *pKa* values, are carried out over a wide range of temperature and concentration using respective modules within COSMOtherm. For *pKa* calculations, respective protonated structures of the molecules were developed using TURBOMOLE. Furthermore, the COSMO-RS related theory and corresponding importance of the simulated properties have been discussed along with the analysis [33].

3. Simulation analysis-results and discussion

3.1. Sigma profile and sigma potential analysis

The molecular interactions of selected solvents with CO_2 play a significant role in dictating the CO_2 solubility. These interactions in turn depend on the shapes, sizes as well as the basic constituent of the molecules involved. The sigma surface of the associated molecules under study i.e. CO_2, H_2O, AEP, APA and TESA are presented in Fig. 1 along with the energy associated with each molecule. Only single conformers with least ground state energy were taken into consideration for the present study. The red, blue and green zones in each of the molecules are credited to the hydrogen bond acceptor, hydrogen bond donor and non-polar area respectively. Probability distribution of composition of surface segment ensemble due to interactions is described by the sigma profile. The sigma profile of the whole system $p_s(\sigma)$ is calculated as a weighted average with mole fraction in the mixture x_i:

$$p_s(\sigma) = \sum_{i\in} x_i \times p_i(\sigma) \tag{1}$$

$pX_i(\sigma)$ is the sigma profile of any molecule X which is presented by:

$$p^{Xi}(\sigma) = \frac{n_i(\sigma)}{n_i} = \frac{A_i(\sigma)}{A_i} \tag{2}$$

where, $n_i(\sigma)$, $A_i(\sigma)$ and A_i are the no. of distributed segments that has surface charge density σ, segment surface area that has charge density σ and area of whole surface cavity rooted in the medium, respectively.

The chemical potential of a surface segment with screening charge density is also a function of normalized distribution which is presented by an implicit equation as:

$$\mu_s(\sigma) = -\frac{RT}{a_{eff}} \ln\left[\int p_s(\sigma') \exp\left(\frac{a_{eff}}{RT}(\mu_s(\sigma') - e(\sigma,\sigma'))\right) d\sigma'\right] \tag{3}$$

where, '$\mu_s(\sigma)$' is a measure for the affinity of the system '*S*' to a surface of polarity 'σ'. Sigma profile and corresponding sigma potential for the molecules which are directive to the structural variations and determine the affinity of solvents to a solute are obtained through simulation and are presented in Fig. 2(a) and (b), respectively.

For σ-scale, positive polarities are represented as negative screening charge density and vice versa. Water being a common

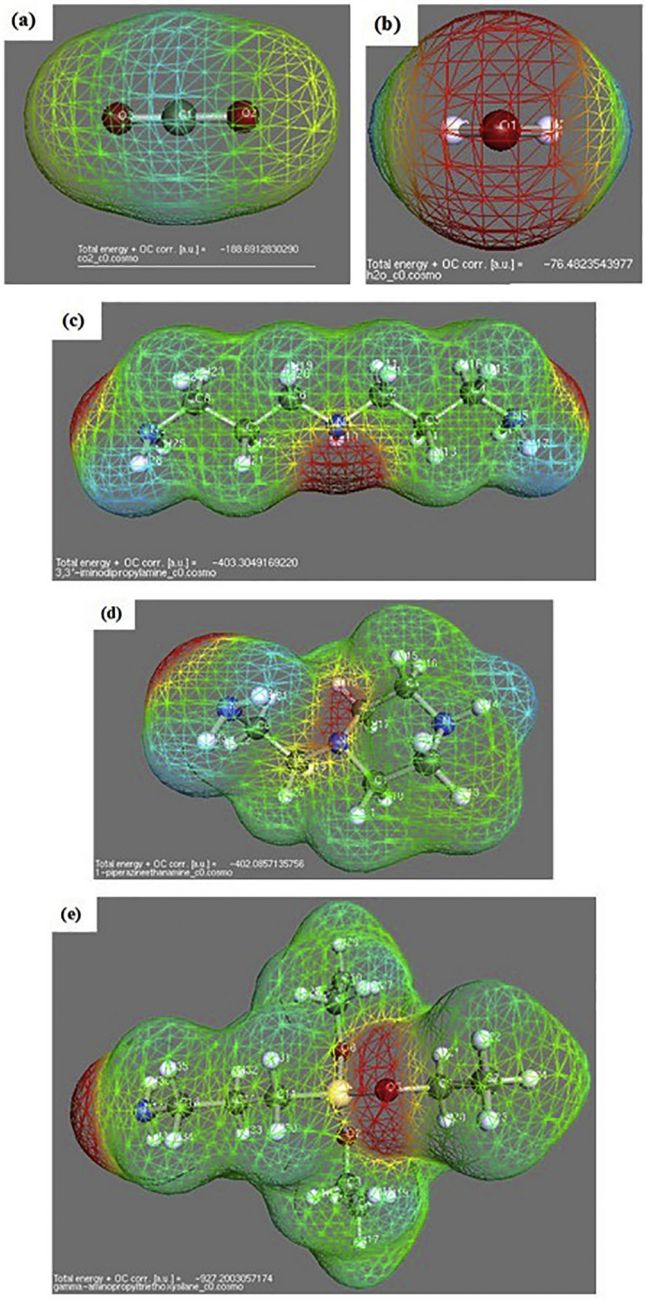

Fig. 1. Sigma surface of (a) CO_2, (b) H_2O, (c) AEP, (d) APA, (e) TESA.

solvent has the extensive range in the sigma profile where $-0.02\ (e/A^2)$ and $+\ 0.02\ (e/A^2)$ indicates the positive polarity of the hydrogen atoms and negative polarity of the oxygen atom in the water molecule, respectively. The water molecule hence is a symmetric molecule where the negative and positive polarities are equivalent. Subsequently, it can also be seen that major part of sigma charge densities of TESA, AEP, APA are negative and that for CO_2 are positive in nature (Fig. 2(a)). This can lead to the conclusion that since CO_2 and the chosen solvents have opposite charge densities or sigma profiles, the solvents may have suitability for CO_2 absorption. This is due to the observation that TESA, AEP and APA have enough negative surface pieces that will interact preferably with positive surface pieces of CO_2. Also, TESA have a slightly more non-polar surfaces than AEP and APA where sigma value is $0\ (e/A^2)$ indicating that TESA should have better CO_2 solubility in comparison to other two solvents. However, from the previous studies the CO_2 solubility in pure TESA is slightly hindered owing to the reason that when TESA reacts with CO_2, it results in formation of a polymeric gel like material [30]. This material is reversible ionic liquid (carbamate anion and cation) with base as TESA and exhibits many of the properties of ILs such as thermal stability. Conclusively, since TESA initially acts as amine and later by reaction with CO_2 acts as IL, its overall experimental solubility is lower in comparison to aq. AEP or APA [7,29].

Sigma potential being a quantity of the response of the solvent to a molecular surface of polarity, it may also provide a qualitative analysis of solvent selection for CO_2 absorption. Sigma potentials associated with both AEP and APA are overlapping in the negative region whereas for the positive σ there is very little variance between the two sigma potentials (Fig. 2(b)). Since, the sigma potential of CO_2 is positive in almost entire range of σ under study with almost a zero potential between the σ range of -0.01 to $+0.01\ (e/A^2)$, the compounds with a more negative potential at a certain σ will attract more CO_2 [34]. CO_2 interactions with AEP/APA are hence expected to be very high along with lower values of activity coefficients in comparison to TESA as an entire entity at equilibrium. The sigma potential profiles corresponding to CO_2 is only symmetrical similar to a parabola in nature whereas for TESA, AEP and APA is more asymmetrical making a major contribution to negative side. With respect to *H*-bonding, TESA, AEP and APA having a negative sigma potential, are able to undergo *H*-bond interactions more in comparison to water which is more saturated with electron donors. Hence, very strong acceptors such as CO_2 in the aqueous phase shall easily undergo *H*-bonding in TESA, AEP and APA solvents corresponding to especially *N* or *O* atoms present in the structures. This is due to the peaks associated with TESA, AEP and APA falling in the region of *H*-bond donor and that of CO_2 in the region of *H*-bond acceptor [35,36]. Consequentially, it can be concluded that CO_2 affinity towards the selected solvent on a molecular level is very much associated to the *H*-bond donor capacity of the solvent. The same concept at reaction engineering level has been previously associated with formation of zwitterions, bicarbonates, unstable/stable bicarbamate, dicarbamates, etc. [7,28,29,34,37]

3.2. Vapor pressure analysis

The concise measurement or evaluation of vapor pressure is extremely important for any carbon capture system. This is owing to the fact that CO_2 solubility either calculated in terms of mole fractions in the liquid phase or in terms of loading i.e. moles of CO_2 per moles of solvent is dependent on the vapor pressure [28]. It also exhibits a huge role in CO_2 solubility via membrane or adsorption processes [38,39]. Solvents exhibiting a lower vapor pressure are considered to be better for CCS applications since these solvents are expected not to enter in the outlet stream through the regeneration section. Another advantage of measurement or efficient prediction of vapor pressures of the blended systems is that they can be further explored for many chemical engineering applications whilst also providing a qualitative understanding of the phase transitions of chemical systems especially comprising of ionic liquids, single or biphasic amine solutions or combination of both. Although, the measurements of vapor pressures do experience a lot of experimental limitations owing to the critical properties of the system and the experimentation being quite costly. Hence, many of the researchers have also focused in critically estimating or modeling the vapor pressure of single or blended solutions for diverse applications.

The concept of combination of zero-pressure fugacity approach along with Peng-Robinson Equation of State (PR-EoS) has been explored by many researchers [40–42] owing to the good predictive capability for vapor pressure. Here, majorly an exponential based temperature function is used as suggested by Soave or Heyen for estimating

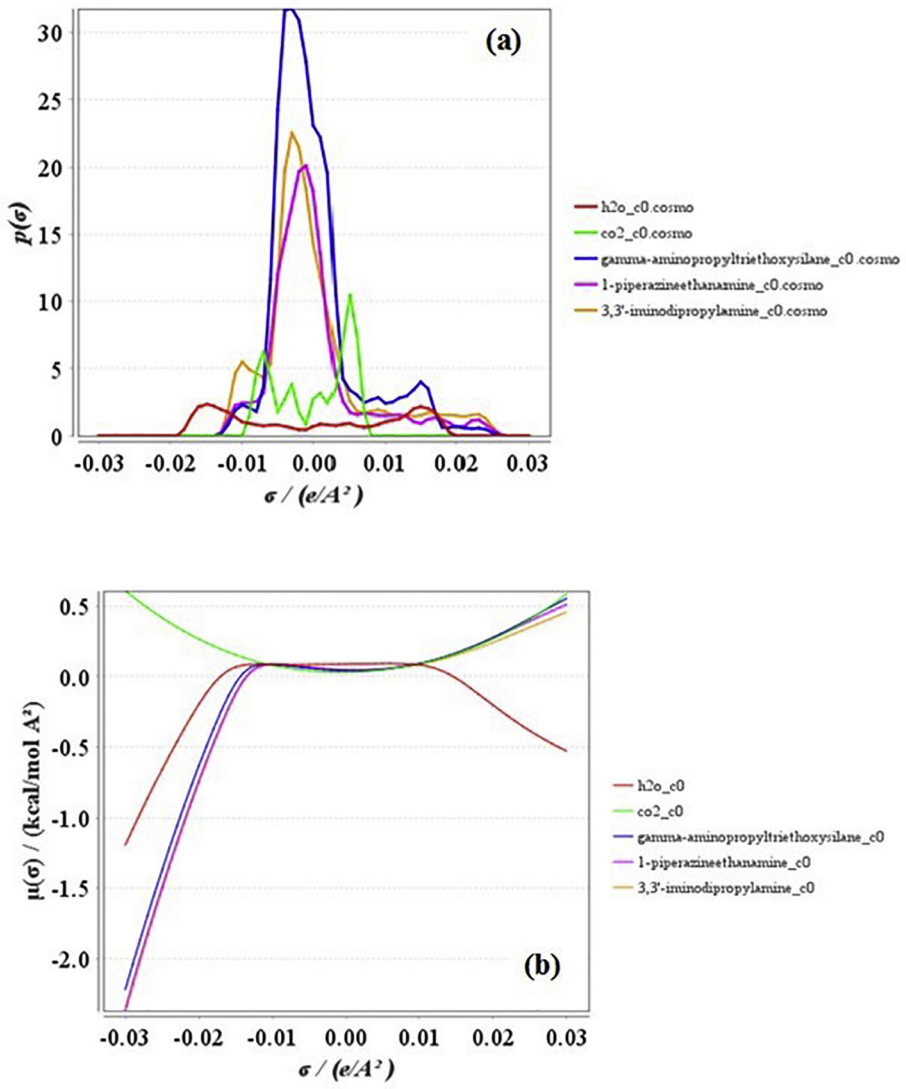

Fig. 2. COSMOtherm generated (a) sigma profile and (b) sigma potential of TESA, H_2O, CO_2, AEP and APA.

vapor pressure through PR-EoS. Novel statistical technique i.e. response surface methodology (RSM) with central composite design where vapor pressure as a function of temperature and composition of the constituent elements has also been applied for the prediction of vapor pressure in the literature [43]. It was found to be very competitive with the actual experimental data of aq. (MDEA + piperazine), aq. (MDEA + [bmim] [BF_4]) and aq. (MDEA+ [bmim] [DCA]) over a wide range of temperature (30–80) C.

The measurement and subsequent modeling of aqueous ionic liquid [emim] [Tf_2N] has been earlier reported in the literature [44] over (323.2–358.2) K and (0.05–0.9) mole fraction of IL as concentration of the system. The authors gave a comparative prediction of UNIFAC-Lei model and COSMO-RS method where the former gave a better prediction and yielding the results closer to the experimental values. The UNIFAC-Lei model is an activity coefficient based model comprising of two components viz. combinatorial and residual.

In the present work, it is being proposed that through the quantum calculations using COSMO-RS, the accurate prediction of vapor pressures can be conceivably achieved. COSMOtherm estimates the vapor pressure of any compound or individual molecule based on the combinatorial and residual contributions similar to UNIFAC-Lei model, through chemical potential calculation of the same as presented in below equation:

$$\frac{p_S^i}{p_{ref}} = \exp\left[-\frac{\left(\mu_{gas}^i - \mu_S^i\right)}{R \times T}\right] \tag{4}$$

where, p_S^i, p_{ref}, μ_{gas}^i, R and T is vapor pressure of the component under study, vapor pressure of the reference component if any considered, the chemical potential of the component in the gas phase, universal gas constant and temperature at which vapor pressure is to be estimated. The vapor pressures were estimated using the inbuilt module for the same, based on the boiling points of the individual pure components of the systems under study as the reference point.

The percentage deviation of all the estimated and experimental quantities have been calculated using equation no. (5):

$$\%AAD = \frac{1}{N} \times \sum_{i=1}^{N} \frac{|Y_i^{exp} - Y_i^{mod}|}{Y_i^{exp}} \times 100 \tag{5}$$

where, N, Y_{exp}^i and Y_{mod}^i, indicate the no. of data points, experimental value and modeled or COSMO estimated value of any variable,

Table 1
Comparison of experimental and COSMO predicted vapor pressure of aq. TESA, aq. (TESA + AEP) and aq. (TESA + APA) systems.

System	Composition ('m'/mol.kg^{-1})	Experimental	Predicted	Experimental	Predicted	Experimental	Predicted	% AAD
	T/K	303.15	303.15	313.15	313.15	323.15	323.15	
aq. TESA	2.432 m	40.7	42.014	65.5	73.417	119.3	123.343	4.231
	1.506 m	41.0	42.128	66.9	73.409	120.7	123.036	
	0.797 m	41.4	42.223	72.4	73.463	121.3	122.967	
aq. (TESA+AEP)	(2.528 + 0.498) m	38.6	40.569	63.4	72.094	110.3	122.621	6.345
	(2.259 + 0.756) m	39.3	40.524	65.5	71.976	118.6	122.365	
	(2.044 + 1.004) m	39.9	40.472	66.9	71.859	119.3	122.129	
aq. (TESA+APA)	(2.528 + 0.499) m	39.3	40.475	64.1	71.927	111.7	122.340	6.922
	(2.259 + 0.753) m	39.3	40.390	64.8	71.738	113.8	121.961	
	(2.044 + 0.991) m	39.9	40.304	65.5	71.559	113.8	121.618	

respectively. All the simulated or calculated values are presented till 3 significant digits after decimal.

The vapor pressures for aq. TESA, aq. (TESA + AEP), and aq. (TESA + APA) systems have been predicted using COSMOtherm and compared with experimental values. The methodology of the measurement of vapor pressure adopted for the present work is described in detail in our previously published work [7,28] (Table 1). The temperature range for comparison is (303.15–323.15) K whereas Antoine equation coefficients are also estimated for all the systems in the temperature range of (298.15–333.15) K (Table 2). The coefficients are found to be a very weak function of temperature and concentration of TESA, AEP or APA owing to the reason of their lower concentration range in the solvents under study. The comparison of the predicted and estimated data indicated a very good agreement for systems aq. TESA, aq. (TESA + AEP) and aq. (TESA + APA) with a low % AAD to be 4.23, 6.35 and 6.92, respectively (Fig. 3). The % AAD are very less in comparison to that mentioned in the literature for similar systems [45,]. Hence, it can be concluded that quantum based vapor pressure calculations are reliable. Also, the discrepancies between the experimental and predicted data is owing to the reason that when vapor pressure is to be measured using experimentation, there exists always few uncertainties associated to maintaining temperature, pressure or formulating the individual composition of the systems whereas while the same has to be predicted through any quantum based chemical calculation, such uncertainties are usually not taken into account.

3.3. Estimation of pure component density and viscosity

Pure component and solution density and viscosity are one of the crucial parameters required for designing the CCS systems which are essential for calculation of pumping costs [46], stripper-absorption tower design [47], calculation of kinetic parameters [48], estimation of excess molar volumes, kinetics deviations which define the system characteristics or their non-ideal behaviour, etc. COSMO-RS estimates density of a pure compound using the corrected molar liquid volume Vi^{-} of the pure compound as per the following equation:

Table 2
COSMO predicted Antoine equation coefficients in aq. TESA, aq. (TESA + AEP) and aq. (TESA + APA) systems.

System	Composition ('m'/mol.kg^{-1})	A	B	C
aq. TESA	2.432 m	19.007	4024.822	−39.556
	1.506 m	19.037	4060.772	−37.681
	0.797 m	19.051	4078.553	−36.723
aq. (TESA +AEP)	(2.528 + 0.498) m	18.171	3497.535	−61.411
	(2.259 + 0.756) m	18.167	3499.427	−61.231
	(2.044 + 1.004) m	18.162	3499.557	−61.154
aq.(TESA+APA)	(2.528 + 0.499) m	18.171	3498.270	−61.387
	(2.259 + 0.753) m	18.167	3500.575	−61.192
	(2.044 + 0.991) m	18.161	3501.189	−61.092

ln(P) = A-(B/(T + C)) (*P* is in mbar and *T* is in K).

$$\rho_i = \frac{M_{Wi}}{\overline{V_i} \times N_A} \tag{6}$$

where, M_{Wi}, N_A and $V_{\bar{i}}$ are the molecular weight of the molecule, Avogadro's number and corrected molar liquid volume, respectively. The latter is computed using Quantitative Structure Property Relationship (QSPR) that comprises of 6 generic QSPR parameters and one element specific parameter. The corrected molar liquid volume is represented as:

$$\overline{V_i} = \left(c_{HMF} \times H_i^{MF}\right) + \left(c_{HHB} \times H_i^{HB}\right) + \left(c_{v\,cos\,mo} \times V_i^{cos\,mo}\right) + \left(c_{M2} \times M_{2i}\right) + \left(c_{Nring} \times N_i^{Ring}\right) + \left(\sum_k^{Elements} c_{AK} \times A_i^k\right) \tag{7}$$

where, H_i^{MF}, H_i^{HB}, V_i^{cosmo}, M_i^2, N_i^{Ring}, A_i^K are pure component misfit interaction enthalpy, hydrogen bonding enthalpy, COSMO volume, second σ-moment, no. of ring atoms and surface area associated with the molecule.

The estimation of viscosity is also based on a QSPR as per the following equation:

$$\ln(\eta i) = (c_{Area} \times A_i) + \left(c_{M2} \times M_i^{\,2}\right) + \left(c_{NRing} \times N_i^{Ring}\right) + (c_{TS} \times TS_i) + c_o \tag{8}$$

where, A_i, M_i^2, N_i^{Ring}, TS_i are surface area, second σ-moment of the compound, number of ring atoms in the compound, and pure component entropy at a specific temperature, respectively. Also, c_{Area}, c_{M2}, c_{NRing},

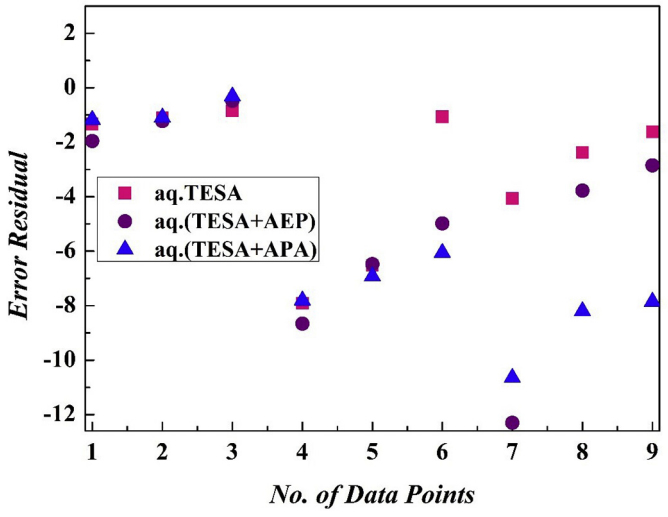

Fig. 3. Residual plot of vapor pressure experimental and COSMO predicted for aq. TESA, aq. (TESA + AEP) and aq. (TESA + APA) system.

Table 3
Comparison of experimental and COSMO predicted density (ρ / kg.m^{-3}) of pure AEP, APA and TESA.

	System					
	AEP		APA		TESA	
Data	ρ_{exp}	ρ_{pred}	ρ_{exp}	ρ_{pred}	ρ_{exp}	ρ_{pred}
T/K						
298.15	980.6	1029.119	928.8	935.558	943.5	954.622
303.15	976.6	1024.414	924.7	931.164	938.8	949.670
308.15	972.5	1019.717	920.6	926.781	934.0	944.748
313.15	968.4	1015.026	916.5	922.410	929.3	939.855
318.15	964.2	1010.342	912.4	918.051	924.5	934.993
323.15	960.2	1005.667	908.3	913.704	919.8	930.160
328.15	956.1	1000.999	904.2	909.369	915.1	925.357
333.15	952.0	996.340	900.1	905.047	910.3	920.583
% AAD	4.799		0.635		1.142	

Table 4
Comparison of experimental and COSMO predicted viscosity (η / mPa.s) of pure AEP and APA.

	System					
	AEP		APA		TESA	
Data	η_{exp}	η_{pred}	η_{exp}	η_{pred}	η_{exp}	η_{pred}
T/K						
298.15	14.48	6.240	8.52	11.460	2.37	6.791
303.15	14.18	5.550	7.00	10.030	2.32	6.027
308.15	11.34	4.955	5.88	8.816	2.21	5.369
313.15	8.67	4.440	5.03	7.781	2.16	4.801
318.15	7.10	3.993	4.61	6.895	1.76	4.308
323.15	5.63	3.602	3.97	6.132	1.61	3.879
328.15	5.04	3.260	3.56	5.474	1.52	3.504
333.15	4.48	2.959	3.13	4.903	1.55	3.174
% 10^{-2} AAD	0.465		0.496		1.416	

c_{TS} and c_o are the generic parameters for the QSPR approach for liquid viscosity with energy values in kcal.mol^{-1} and areas in [Å^2].

The methodology accepted and the uncertainties associated with the measurements of density and viscosity is discussed in our previous work [28]. A comparison of experimental and COSMOtherm predicted density and viscosity of pure AEP, APA and TESA is carried out in the present work (Tables 3 and 4). The prediction of density exhibits a low deviation. The major difference between the COSMOtherm predicted density or viscosity is the dependence of the variable according to QSPR which is taken to be independent of temperature. However, while comparing the experimental and predicted viscosity for all the systems under consideration, either under estimation or over estimation is observed through COSMO resulting an overall a very high % AAD. Similar observations were also reported elsewhere [49].

3.4. Infinite dilution activity coefficients

The operation of absorption / stripping columns used in post combustion CO_2 capture processes require quite a knowledge about infinite dilution activity coefficients (IDACs) of the corresponding mixtures. It also represents the extent of non ideality in liquid solvents. Various thermodynamic properties in turn also depend on the values of activity coefficients. IDACs are also useful in determining the partition coefficients, separation factors as well as for Henry's constant. Since IDACs might be very difficult to obtain owing to the high experimental costs associated with them, for prior screening of solvents, an appropriate prediction of the variable may provide useful insight to the system [50–52]. Many different approaches have already been reported in the literature such as original and modified UNIFAC which works on the group contributions of the associated molecules [53].

For COSMO calculations, the activity coefficient at infinite dilution estimation is based on chemical potential of the associated compound which in turn depends on the surface change density and is obtained by:

$$\ln \gamma_i^{\infty} = \frac{\mu_i^{\infty} - \mu_i^{0}}{R \times T} \tag{9}$$

where, T^{∞}, μ_i^{∞}, μ_i^{0} are activity coefficient of compound *'i'* at infinite dilution, pseudo-chemical potential of *'i'* at infinite dilution and chemical potential of *'i'* in its pure liquid state, respectively. The efficient prediction of IDACs through COSMOtherm and comparison of the same with the experimental data has been reported in the literature for aqueous, non-aqueous, organic, or IL systems [52]. One of the major advantage reviewed from the literature for estimation of IDACs through COSMOtherm is due to the absence of mean field approximation in thermodynamic estimation of IDACs.

COSMO based prediction of activity coefficients of TESA, AEP and APA in H_2O as a function of temperature in range of (298.15–333.15) K is carried out in the present work (Table 5). With rise in temperature IDACs of TESA, AEP and APA in water were found to increase. Although the IDACs of TESA are very high in comparison to the values of AEP and APA. The IDACs having values greater than unity are found to decrease with temperature and those having less than a unit value tend to rise with temperature. Similar trends are also observed for thiophene and ILs systems [36]. A higher value indicating non-polarity of the compound of interest in the solvent under consideration whereas a lower value represents active polarity of the compound in the system. The IDACs for any binary system if equals to unity, the binary pair then can be considered to be an ideal one. Whereas for the present cases, all the IDACs are greater or less than unity indicating a highly non-ideal behaviour of such systems.

Table 5
COSMO predicted Activity Coefficient of TESA, AEP, and APA at infinite dilution in water.

	T/K	298.15	303.15	308.15	313.15	318.15	323.15	328.15	333.15
T^{∞}	TESA	17.108	24.099	33.161	44.607	58.705	75.643	95.499	118.213
	AEP	0.231	0.293	0.368	0.45	0.558	0.675	0.808	0.957
	APA	0.011	0.015	0.019	0.025	0.031	0.040	0.049	0.062

3.5. Vapor liquid equilibrium analysis of (TESA + H_2O), (TESA + H_2O + CO_2), (TESA + H_2O + AEP), and (TESA + H_2O + APA) through estimation of activity coefficient, chemical potential, excess Gibb's and enthalpy

In a chemically reacting system, the distribution or formation of individual species and/or constituent molecules at a particular temperature and pressure is dictated by the chemical potential which in turn is dependent on the values of Gibbs free energy. The temperature dependence of excess Gibbs free energy is further explained through calculation of excess enthalpy. The activity coefficient of any solvent is highly appreciated for acid- gas separation system since it is one of the variables indicating the maximum gas solubility which can be achieved at equilibrium. The chemical potential i.e. both external chemical potential and internal chemical potential, are also attributed to different energies associated with any molecule. For e.g. the internal chemical potential is designated by temperature, density, internal energy and enthalpy of any molecule/compound. Due to this, a very close relationship exist amongst the major thermodynamic properties, evaluation of which may yield an important insight to the system. Additionally, energetic investigation on the enthalpy effects due to certain intermolecular interactions amid CO_2 and proposed solvents is capable to explain the performance of CO_2 solubility. Henceforth, the vapor liquid equilibrium of the binary and ternary mixtures of aq. TESA, aq. (TESA + CO_2), aq. (TESA + AEP), and aq. (TESA + APA) which

incorporates the non-linear relationship between the individual constituents is computed using the COSMO-RS theory. This is further quantified in terms of activity coefficients, excess Gibbs free energy, excess enthalpy, chemical potential and individual partial pressures associated with the system at 303.15, 313.15 and 323.15 K. The total pressure of the systems of aq. (TESA), aq. (TESA + AEP) and aq. (TESA + APA) is (0–43) mbar whereas for aq. (TESA + CO_2) it is (0–93) bar. This is owing to the reason that in the latter case, involvement of a gas phase is high. Along with this, the COSMO calculated activity coefficient (or VLE) values are further related to NRTL, WILSON and UNIQUAC 4 models and corresponding error is presented in RMSD form using the following equation:

$$RMSD = \sqrt{\frac{\sum_{i=1}^{n} (y_{COSMO} - y_i)^2}{n}} \tag{10}$$

Where y_{COSMO} is COSMO predicted property and y_i is NRTL, WILSON or UNIQUAC predicted property value. The binary interaction parameters of the models are also obtained for all the systems under study.

A brief description of each model is stated in the below section [33].

3.5.1. Conductor like screening model (COSMO)

The COSMO model defining the VLE of any system is based majorly on the following equations:

$$\gamma_S^{Xi} = \exp\left(\frac{\mu_s^{Xi} - \mu_{Xi}^{Xi}}{RT}\right) \tag{11}$$

$$P^{tot} = \sum_i P_{vap}^{Xi} x_i \gamma_S^{Xi} \tag{12}$$

$$y_i = \frac{P_{vap}^{Xi} x_i \gamma_S^{Xi}}{P^{tot}} \tag{13}$$

P^{tot}, x_i, and y_i is the total vapor pressure of the mixture, mole fraction of the compounds in liquid phase, mole fraction of compounds in gas phase, respectively. Therefore, The VLE estimation through COSMO is based on the vapor pressures and activity coefficients of individual pure constituents in the mixture.

3.5.2. Non-random two-liquid model (NRTL)

The estimation of activity coefficients as a function of excess Gibbs free energy for any system (binary in the present case) is done through NRTL model which is based on the local concentration of individual chemical constituents or electrolytic ionic species [54] and is described by the following equations [55]:

$$\ln(\gamma_i) = \frac{\sum_j x_j \tau_{ji} G_{ji}}{\sum_k x_k G_{ki}} + \sum_j \frac{x_i G_{ij}}{\sum_k x_k G_{kj}} \left[\tau_{ij} - \frac{\sum_m x_m \tau_{mj} G_{mj}}{\sum_k x_k G_{kj}}\right] \tag{14}$$

$$G_{ij} = \exp(-\alpha_{ij} \tau_{ij}) \tag{15}$$

For each binary system, there are three amendable parameters of the NRTL equation namely τ_{ij}, τ_{ji}, $\alpha = \alpha_{ij} = \alpha_{ji.}$ τ_{ij} and τ_{ji} are the binary interaction parameters of the associated constituents. The non-randomness factor α which signifies the molecule-molecule or molecule-electrolyte (if any) in the system is taken to be having the default value of 0.3.

3.5.3. WILSON model

The activity coefficient for any given system through non-linear least square regression analysis of WILSON equation which can be estimated by:

$$\ln(\gamma_i) = 1 - \ln\left(\sum_k x_k \lambda_{ik}\right) - \sum_j \frac{x_k \lambda_{ji}}{\sum_k x_k \lambda_{jk}} \tag{16}$$

$$\Omega_{ij} = \lambda_{ji} = \frac{V_i}{V_j} \exp\left[-\frac{a_{ji}}{RT}\right] \tag{17}$$

where, λ_{ij}, λ_{ji}, V_i, V_j, a_{ji}, and a_{ij} are binary interaction parameters of the system under study.

3.5.4. Universal Quasichemical model (UNIQUAC 4)

In case of UNIQUAC 4 model, the activity coefficients are calculated using both the combinatorial and residual contributions associated with the molecules. The model is as by large in simple terms is presented as:

$$\ln(\gamma_i) = \ln(\gamma_i^C) + \ln(\gamma_i^R) \tag{18}$$

where the first term $\ln(\Upsilon_i^C)$ is the combinatorial contribution and represents the entropic size and shape transformations of the compounds. The contribution is further equated as:

$$\ln(\gamma_i^C) = \ln\left(\frac{\phi_i}{x_i}\right) + \frac{z}{2} q_i \ln\left(\frac{\Theta_i}{\phi_i}\right) + l_i - \frac{\phi_i}{x_i} \sum_j x_j l_j \tag{19}$$

where, Φ_i and Θ_i are normalized volume and surface area fraction of species 'i' in the blended solvent. Furthermore, these parameters are related to the mole fractions 'x_i', volume 'r_i' and surface area 'q_i' for each individual species. The parametric equations are given below:

$$\phi_i = \frac{x_i r_i}{\sum_j r_j x_j} \tag{20}$$

$$\Theta_i = \frac{x_i q_i}{\sum_j q_j x_j} \tag{21}$$

$$l_i = \frac{z}{2}(r_i - q_i) - (r_i - 1) \tag{22}$$

The enthalpy interactions amongst various constituents in UNIQUAC 4 model is quantified by the residual contribution in calculation of the activity coefficient. The said term is described as:

$$\ln(\gamma_i^R) = q_i \left[1 - \ln\left(\sum_j \Theta_j \tau_{ji}\right) - \sum_j \frac{\Theta_j \tau_{ij}}{\sum_k \Theta_k \tau_{kj}}\right] \tag{23}$$

Table 6
COSMO predicted NRTL model parameters for the activity coefficients in (H_2O (1) + TESA (2)) system.

System	T / K	α	τ_{12}	τ_{21}	*rmsd*
H_2O(1) + TESA(2)	303.15	0.3	5.313	−1.462	0.192
	313.15	0.3	5.543	−1.285	0.176
	323.15	0.3	5.735	−1.115	0.166

Table 7
COSMO predicted WILSON model parameters for the activity coefficients in (H_2O (1) + TESA (2)) system.

System	T/K	λ_{12}	λ_{21}	a_{12}	a_{21}	v_1	v_2	*rmsd*
H_2O	303.15	2.547	0.008	−2.049	4.385	25.855	304.606	0.292
(1) + TESA	313.15	2.175	0.006	−2.018	4.688	25.855	304.606	0.283
(2)	323.15	1.868	0.005	−1.985	4.985	25.855	304.606	0.278

Table 8
COSMO predicted UNIQAC 4 model parameters for the activity coefficients in (H_2O (1) + TESA (2)) system.

System	T/K	q_1	q_2	r_1	r_2	τ_{12}	τ_{21}	u_{12}	u_{21}	a_{12}	a_{21}	rmsd
H_2O(1) + TESA(2)	303.15	6.278	13.863	4.126	19.248	1.243	2.235	−0.131	−0.484	−66.010	−243.779	0.191
	313.15	1.771	5.071	1.164	7.041	1.805	0.869	−0.368	0.087	−184.979	43.786	0.174
	323.15	1.599	5.291	1.051	7.346	1.902	0.621	−0.413	0.307	−207.675	154.233	0.158

Table 9
COSMO predicted NRTL parameters for the activity coefficients in (H_2O (1) + TESA (2) + CO_2 (3)), (H_2O (1) + TESA (2) + AEP (3)) and (H_2O (1) + TESA (2) + APA (3)) systems.

System	aq. (TESA + CO_2)			aq.(TESA + AEP)			aq.(TESA + APA)		
T/K	303.15	313.15	323.15	303.15	313.15	323.15	303.15	313.15	323.15
α	0.3	0.3	0.3	0.3	0.3	0.3	0.3	0.3	0.3
τ_{12}	5.450	5.569	5.668	4.581	4.723	4.835	4.472	4.658	4.797
τ_{13}	3.769	3.761	3.757	−0.221	−0.126	−0.020	0.454	0.644	0.867
τ_{21}	−1.839	−1.675	−1.517	−1.514	−1.357	−1.205	−1.457	−1.307	−1.159
τ_{23}	−2.379	−2.339	−2.299	0.330	0.271	0.222	0.497	0.406	0.316
τ_{31}	6.766	6.639	6.516	−1.980	−1.845	−1.719	−3.124	−3.019	−2.925
τ_{32}	1.875	1.828	1.781	−0.043	−0.004	0.031	0.603	0.661	0.729
rmsd	0.371	0.357	0.346	0.328	0.307	0.288	0.360	0.329	0.302

Table 10
COSMO predicted WILSON parameters for the activity coefficients in (H_2O (1) + TESA (2) + CO_2 (3)), (H_2O (1) + TESA (2) + AEP (3)) and (H_2O (1) + TESA (2) + APA (3)) systems.

System	aq. (TESA + CO_2)			aq.(TESA + AEP)			aq.(TESA + APA)		
T/K	303.15	313.15	323.15	303.15	313.15	323.15	303.15	313.15	323.15
λ_{12}	3.886	3.406	2.994	2.725	2.405	2.121	2.260	2.092	1.892
λ_{13}	0.004	0.005	0.626	4.509	4.085	3.726	8.514	7.843	7.238
λ_{21}	0.000	0.000	0.000	0.013	0.008	0.006	0.037	0.016	0.009
λ_{23}	0.063	0.067	0.712	0.979	0.915	0.855	0.412	0.425	0.417
λ_{31}	0.103	0.105	0.107	1.832	1.695	1.549	1.768	1.586	1.412
λ_{32}	8.433	8.258	8.813	0.769	0.852	0.930	0.650	0.676	0.720
a_{12}	−2.304	−2.297	−2.288	−2.089	−2.081	−2.067	−1.977	−1.994	−1.993
a_{13}	2.914	2.887	2.856	−2.073	−2.079	−2.087	−2.507	−2.539	−2.568
a_{21}	10.161	9.261	9.513	4.113	4.519	4.884	3.473	4.117	4.637
a_{23}	2.772	2.827	2.879	0.333	0.387	0.442	0.803	0.810	0.849
a_{31}	1.745	1.792	1.839	0.801	0.876	0.961	0.873	0.969	1.076
a_{32}	−2.394	−2.459	−2.524	−0.163	−0.231	−0.295	−0.009	−0.034	−0.076
v_1	25.855	25.855	25.855	25.855	25.855	25.855	25.855	25.855	25.855
v_2	304.606	304.606	304.606	304.606	304.606	304.606	304.606	304.606	304.606
v_3	48.329	48.329	48.329	178.942	178.942	178.942	194.863	194.863	194.863
rmsd	0.401	0.381	0.362	0.362	0.333	0.307	0.430	0.386	0.346

Table 11
COSMO predicted UNIQUAC 4 parameters for the activity coefficients in (H_2O (1) + TESA (2) + CO_2 (3)), (H_2O (1) + TESA (2) + AEP (3)) and (H_2O (1) + TESA (2) + APA (3)) systems.

System	aq. (TESA + CO_2)			aq.(TESA + AEP)			aq.(TESA + APA)		
T / K	303.15	313.15	323.15	303.15	313.15	323.15	303.15	313.15	323.15
q_1	1.803	1.816	1.810	20.120	17.307	14.230	6.484	5.916	5.117
q_2	4.426	4.417	4.775	71.680	65.279	56.582	22.562	21.371	19.042
q_3	1.687	1.834	1.985	82.585	70.859	58.260	35.128	32.469	28.868
r_1	1.185	1.193	1.189	13.222	11.373	9.351	4.261	3.888	3.362
r_2	5.613	6.132	6.629	99.527	90.640	78.564	31.328	29.674	26.439
r_3	1.739	1.891	2.466	111.079	95.308	78.361	44.503	41.134	36.572
τ_{12}	2.329	2.288	2.229	1.097	1.082	1.062	1.056	1.026	0.985
τ_{13}	0.458	0.531	0.605	1.189	1.192	1.198	1.462	1.451	1.454
τ_{21}	0.771	0.687	0.625	2.635	2.622	2.605	2.439	2.410	2.368
τ_{23}	3.743	3.539	3.374	1.114	1.157	1.219	1.582	1.591	1.608
τ_{31}	0.115	0.128	0.132	2.425	2.407	2.379	1.869	1.849	1.806
τ_{32}	0.125	0.148	0.170	0.890	0.853	0.801	0.536	0.531	0.519
u_{12}	−0.509	−0.515	−0.515	−0.056	−0.049	−0.038	−0.033	−0.016	0.009
u_{13}	0.471	0.394	0.323	−0.104	−0.109	−0.116	−0.229	−0.232	−0.241
u_{21}	0.157	0.234	0.302	−0.584	−0.599	−0.615	−0.537	−0.547	−0.553
u_{23}	−0.795	−0.786	−0.781	−0.065	−0.091	−0.127	−0.276	−0.289	−0.305
u_{31}	1.304	1.280	1.299	−0.534	−0.547	−0.557	−0.377	−0.383	−0.379
u_{32}	1.252	1.188	1.138	0.070	0.099	0.143	0.376	0.394	0.421
a_{12}	−256.343	−259.186	−258.995	−27.928	−24.753	−19.289	−16.533	−8.137	4.939
a_{13}	236.927	198.314	162.306	−52.486	−55.064	−58.470	−115.063	−116.579	−121.058
a_{21}	78.905	117.651	151.730	−293.762	−301.870	−309.343	−270.345	−275.473	−278.504
a_{23}	−400.105	−395.752	−392.989	−32.795	−45.777	−64.124	−139.057	−145.343	−153.422
a_{31}	655.969	644.306	654.106	−268.559	−275.021	−280.042	−189.708	−192.595	−190.992
a_{32}	629.866	597.646	572.706	35.178	49.925	71.867	189.141	198.403	211.972
rmsd	0.172	0.158	0.146	0.264	0.244	0.226	0.308	0.280	0.254

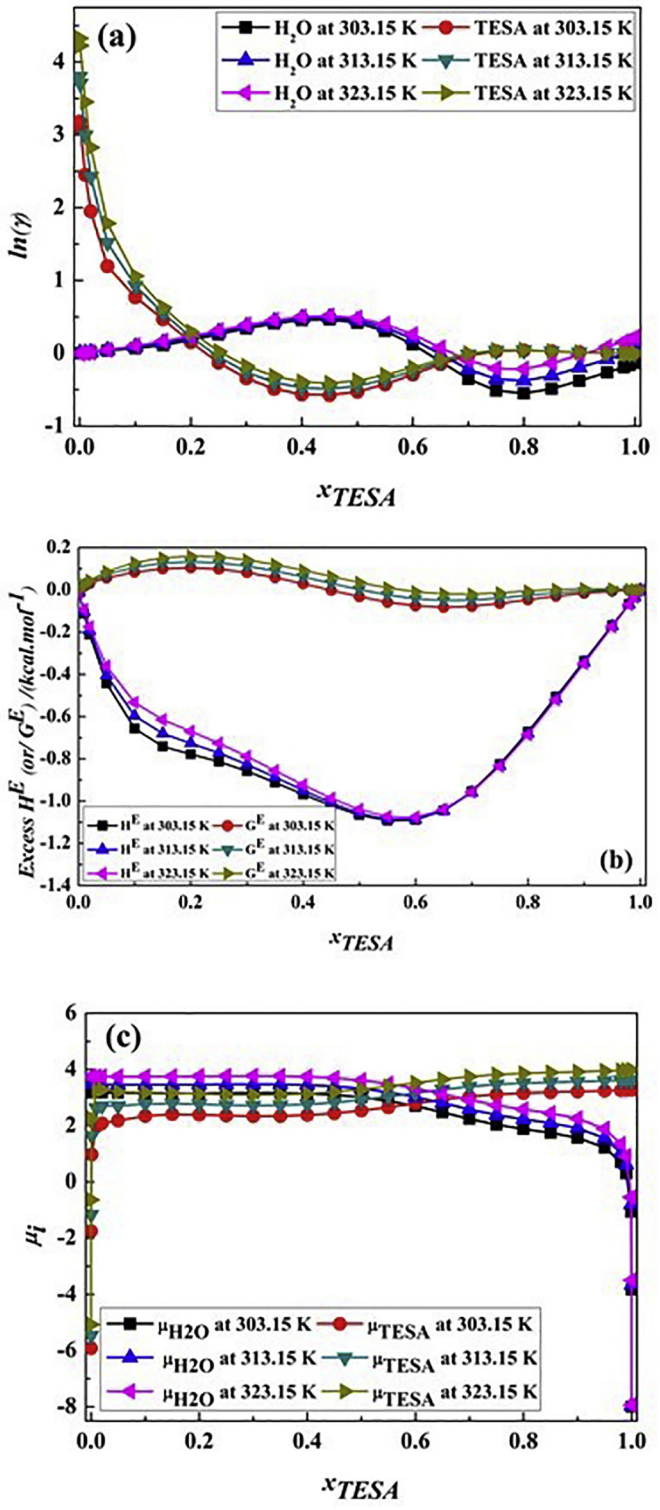

Fig. 4. COSMO predicted (a) Activity coefficient (b) Excess enthalpy and Gibb's free energy (c) Chemical potential as a function of mole fraction of TESA for aq. TESA system.

Enthalpy being closely related to temperature, the residual contribution binary interaction major parameters 'τ_{ij}' are further taken as an inverse logarithm function of temperature and the same is given as:

$$\ln(\tau_{ij}) = -\frac{\Delta u_{ij}}{RT} = -\frac{a_{ij}}{T} \tag{24}$$

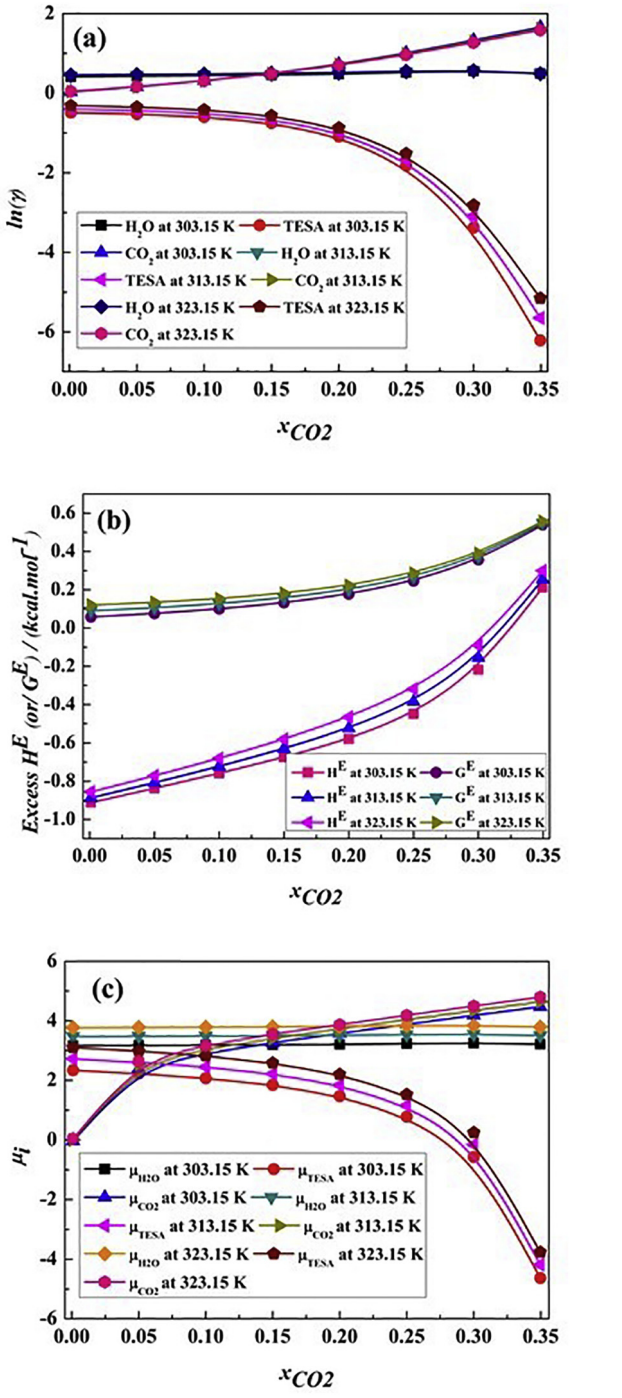

Fig. 5. COSMO predicted (a) Activity coefficient (b) Excess enthalpy and Gibb's free energy (c) Chemical potential as a function of mole fraction of CO_2 for aq. (TESA + CO_2) system at $x_{H2O} = 0.65$.

The compound specific UNIQUAC volume and surface area parameters are given by:

$$r_i = \frac{s_i V_i^{COSMO}}{30} \tag{25}$$

$$q_i = \frac{s_i A_i^{COSMO}}{40} \tag{26}$$

Involved activity coefficients and binary interaction parameters for NRTL, WILSON and UNIQUAC 4 models were estimated (Tables 6–11).

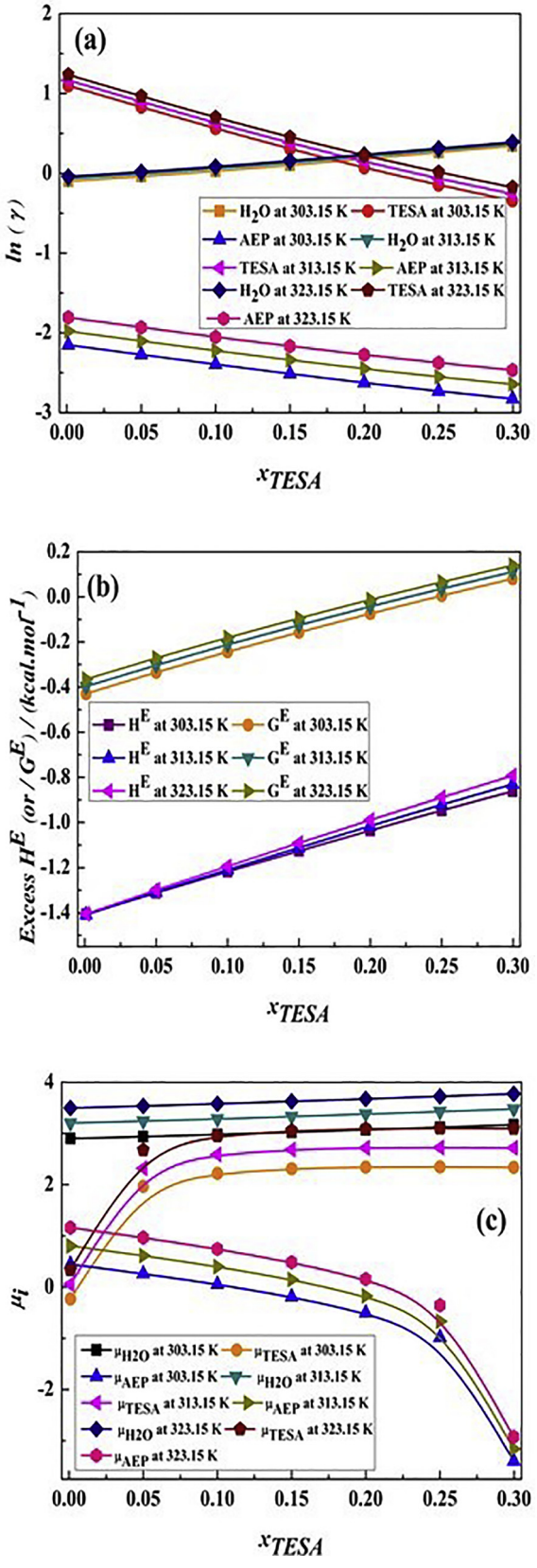

Fig. 6. COSMO predicted (a) Activity coefficient (b) Excess enthalpy and Gibb's free energy (c) Chemical potential as a function of mole fraction of TESA for aq. (TESA + AEP) system at $x_{H2O} = 0.70$.

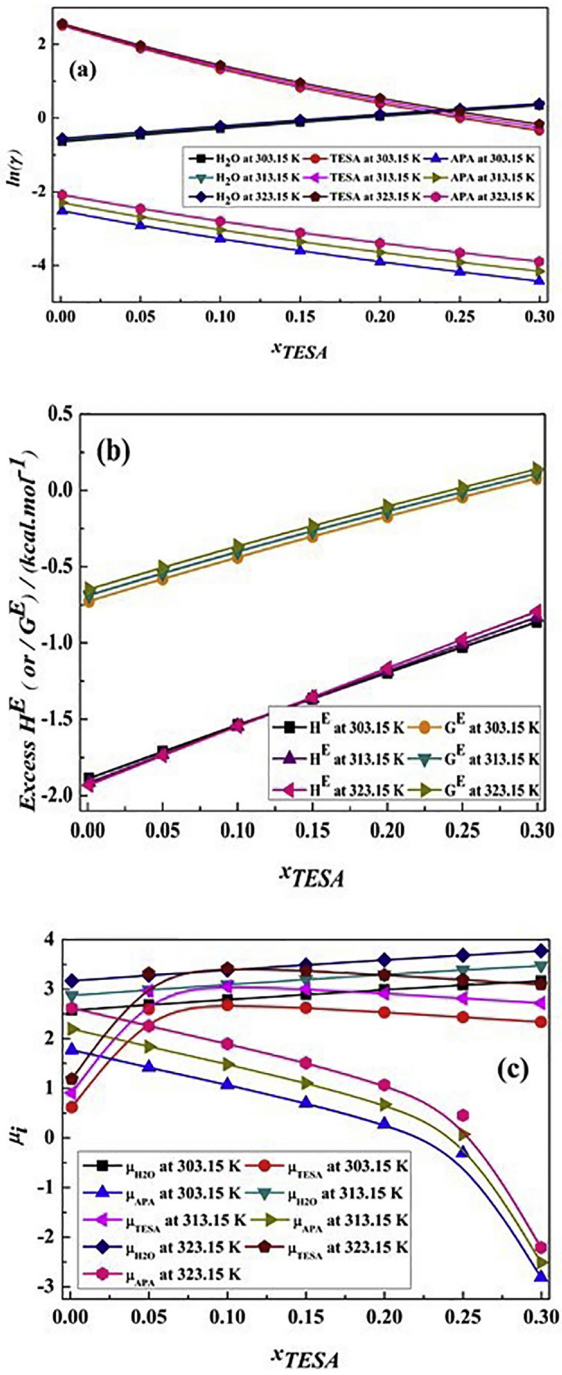

Fig. 7. COSMO predicted (a) Activity coefficient (b) Excess enthalpy and Gibb's free energy (c) Chemical potential as a function of mole fraction of TESA for aq. (TESA + APA) system at $x_{H2O} = 0.7$.

All the observed systems modeled using the methods are asymmetric in nature owing to the different values of the major binary interaction parameters. i.e. ($\tau_{ji} \neq \tau_{ij}$).

The activity coefficients of TESA in aq. TESA system is found to first exhibit a steep decrease and concurrently for H_2O a slight increase till $x_{TESA} = 0.4$ was observed. The property was found to exhibit almost a similar value for H_2O over a wide range of TESA concentration though (Fig. 4(a)). A very slight deviations of ln (γ), H^E (excess enthalpy), G^E

Table 12
COSMO predicted CO_2 solubility ($100 \times x$) from (1.0–3.0) bar pressure in temperature range of (303.15–323.15) K*.

		T/K				T/K				T/K		
aq. TESA/(mol.kg^{-1})	P/bar	303.15	313.15	323.15	(TESA + AEP)/(mol.kg^{-1})	303.15	313.15	323.15	(TESA + APA)/(mol.kg^{-1})	303.15	313.15	323.15
2.432	1.0	0.083	0.070	0.060	2.528 + 0.498	0.096	0.081	0.069	2.528 + 0.499	0.096	0.081	0.069
	1.5	0.124	0.104	0.089		0.143	0.120	0.103		0.144	0.121	0.104
	2.0	0.165	0.139	0.119		0.190	0.160	0.137		0.191	0.161	0.138
	2.5	0.205	0.173	0.148		0.237	0.200	0.171		0.238	0.201	0.172
	3.0	0.246	0.207	0.178		0.284	0.239	0.205		0.285	0.240	0.206
1.506	1.0	0.054	0.046	0.039	2.259 + 0.756	0.092	0.077	0.066	2.259 + 0.753	0.092	0.078	0.066
	1.5	0.081	0.069	0.059		0.137	0.115	0.099		0.138	0.116	0.099
	2.0	0.108	0.091	0.078		0.182	0.153	0.131		0.183	0.154	0.132
	2.5	0.135	0.114	0.098		0.227	0.191	0.164		0.228	0.192	0.165
	3.0	0.162	0.136	0.117		0.271	0.229	0.196		0.273	0.230	0.197
	1.0	0.037	0.031	0.026		0.089	0.075	0.064		0.090	0.075	0.065
	1.5	0.055	0.046	0.039		0.133	0.112	0.096		0.134	0.113	0.097
	2.0	0.073	0.061	0.052		0.177	0.149	0.128		0.178	0.150	0.129
	2.5	0.091	0.076	0.065		0.221	0.186	0.160		0.222	0.187	0.160
	3.0	0.109	0.091	0.078		0.264	0.223	0.191		0.266	0.224	0.192

* x is the mole fraction of CO_2 in the loaded solvent.

(excess Gibbs free energy) and μ with respect to temperature change from 303.15 to 323.15 K is observed as shown in Fig. 4. However, the properties are found to be a function of TESA concentration. Further, for H^E all the values observed are either 0 or -*ve* in nature exhibiting a minima near at $x_{TESA} = 0.6$ and G^E values are observed to be slightly +*ve* till $x_{TESA} = 0.5$ parade by –*ve* nature. The negative G^E indicates the spontaneous mixing because of the thermodynamic driving forces between the two components. Corresponding chemical potentials were also found to slightly increase with temperature and have minimal values at infinite dilutions of the system. i.e. at $x_{TESA} \approx 0$ and $x_{H2O} \approx 0$ as presented in Fig. 4 (c). The results of vapor liquid equilibrium relationship of aq. (TESA + CO_2) system at $x_{H2O} \approx 0.65$ in presented in Figs. 5. The results are preferred at $x_{H2O} \approx 0.65$ owing to the fact that most of the developed amine technology attempts to use a solvent concentration ranging between 25 and 40% and hence the elected concentration of TESA may provide useful insights to the technology. Comparing Figs. 4 and 5, it is realized that the chemical potential of TESA in aq. TESA system is much higher which then gets reduced when it reacts with CO_2 since chemical potentials of any compound has a tendency to move from a high value to lower one. Hence, the internal energy associated in aq. TESA system which is particularly associated with TESA gets released in form of free energy while TESA reacts with CO_2 forming various intermediate or final species such as bicarbamate, bicarbonates, protonated hydrogen, etc. This also suggest that CO_2 has major affinity towards TESA rather than water which is also proved in literature [30–32]. Also, G^E for the system aq. (TESA + CO_2) is +*ve* which indicates an external force is required in order to mix CO_2 with aq. TESA. Usually, this force is applied through the changes in partial pressures of CO_2 and temperature as per Le-Chatelier's principle while carrying out the experimental VLE study. Whereas, H^E is -*ve* for both aq. TESA and aq. (TESA + CO_2) system indicting an exothermic reaction / mixing in both the systems which is proven by the values of heat of absorption [56,57].

Furthermore, the vapor liquid equilibrium analysis comprising of activity coefficients, excess enthalpy, excess Gibbs' free energy and chemical potentials of aq. (TESA + AEP) and aq. (TESA + APA) at high H_2O concentration ($x_{H2O} \approx 0.70$) is presented in Figs. 6 and 7, respectively.

The G^E at the studied H_2O concentration is found to be both –*ve* and + *ve* in nature as a function of TESA concentration indicating that external force is required to be applied in order to achieve uniform mixing at a given concentration of AEP and TESA. This is also very similar to the physically observed mixing since the viscosity of AEP is quite high in comparison of TESA and H_2O and hence mixing requires some extra manual force in comparison to non-viscous solution [27]. The positive nature of H^E also indicates the same being an endothermic reaction / process. Chemical potentials of aq. (TESA + AEP/APA) at high concentration of water for all the chemical constituents were found to be rising with increase in temperature. Nevertheless, the chemical potential of H_2O was obtained to be +*ve* indicating its major contribution to the system. The chemical potentials of TESA and AEP/APA were attained to be high comparatively till $x_{TESA} \approx 0.5$. The chemical potentials were observed to be in the order: $\mu_{H2O} > \mu_{AEP/APA} > \mu_{TESA}$.

3.6. CO_2 solubility in aq. TESA, aq. (TESA + AEP) and aq. (TESA + APA)

CO_2 solubility over a wide range of temperatures and CO_2 partial pressures is of great importance in post and pre-combustion processes. However, for mostly post combustion processes lower pressures studies are important attributing to the lean concentration of CO_2 in flue gas streams. Hence, in the current study CO_2 solubility in the solvents was simulated and obtained over (303.15–323.15) K at (1.0–3.0) bar solute pressure with an increment of 0.5 bar. The gas solubility is calculated as:

$$p_j = p_j^0 \times x_j \times \gamma_j \tag{27}$$

where p_j^0, γ_j, x_j, and p_j are vapor pressure of pure compound, activity coefficient, mole fraction, and partial pressure, respectively, of compound '*j*'. The actual CO_2 solubilities in the studies solvents may differ from the simulated which can be further acknowledged to various parameters effecting the process: vapor pressures, temperature, or maintenance of the partial pressure in the system. Also, while estimating through COSMOtherm, the gas is assumed to be ideal that is fugacity coefficient associated is considered to be unity whereas in practical work, the fugacity of the systems are usually less than unity [28]. The solubilities are presented in terms of mole fraction of CO_2 in the liquid phase (x_{CO2}).The results are being presented in Tables 12. The results are very much indicating that increasing the AEP/APA concentration in aq. TESA solutions, CO_2 solubility increases. Simultaneously, inverse relationship between CO_2 solubility and temperature is also observed. Qualitatively, APA is still a better activator when compared to AEP for aqueous systems as well as when compared to blended aq. TESA system.

3.7. Henry's constant H_{CO2} and H_{N2O} in aq. TESA, aq. (TESA + AEP) and aq. (TESA +APA) systems

The contribution of physical solubility of any gas in a proposed solvent can be evaluated through henry's law constant. For CO_2 capture system, usually, the same is either measured experimentally or estimated through various empirical correlations available [48,59].

Analytically, the henry's law coefficient is calculated through the chemical potential difference between the ideal gas phase and the

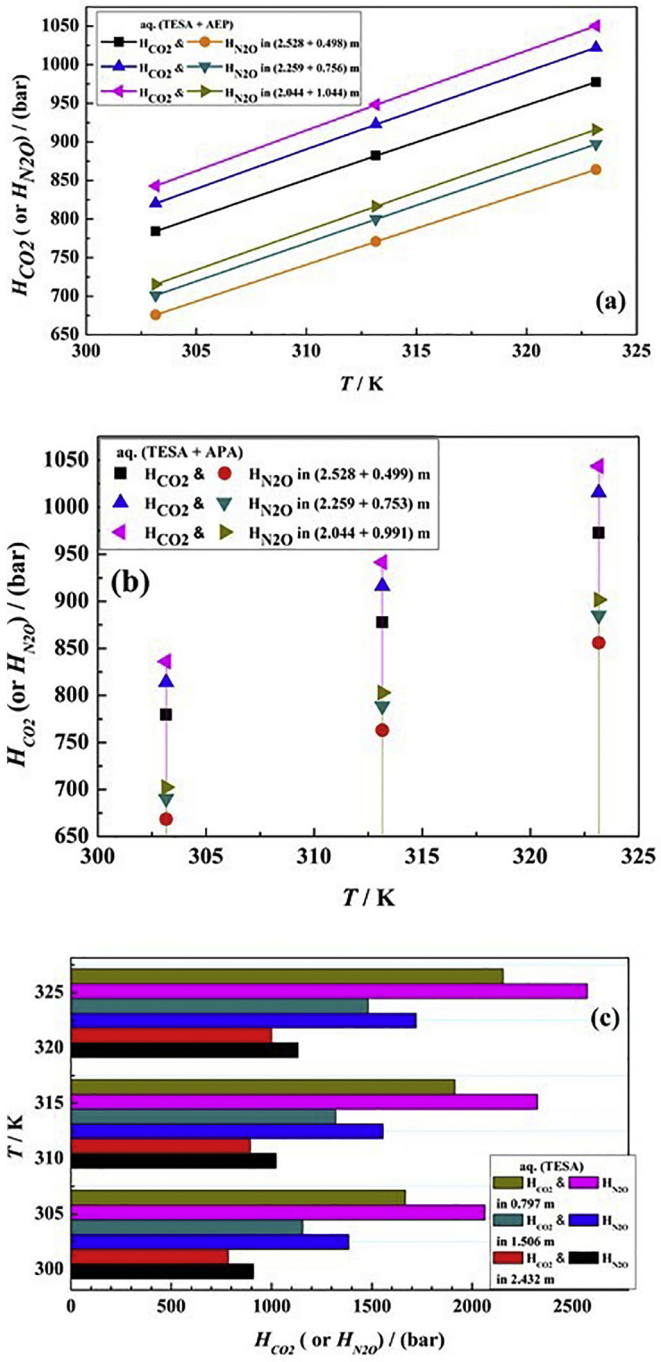

Fig. 8. COSMO predicted Henry's Constant of CO_2 and N_2O in (a) aq. (TESA + AEP), (b) aq. (TESA + APA) and (c) aq. (TESA) systems as a function of composition and temperature.

Table 14
pKa values of AEP and APA at 298.15 K in various solvents.

	Solvent	H_2O	Acetonitrile	Tetrahydrofuran
pKa	AEP	5.2939	13.2832	9.7851
	APA	5.2549	13.2692	9.7605

infinite dilution state in the given solvent or solvent mixture. Whereas, for an incompressible liquid the law coefficient is the product of the infinite dilution activity coefficient and pure compound vapor pressure. The mathematical representation of the same is as below:

$$H_j^s = \left[\frac{\left(\mu_j^{s,\infty} - \mu_j^{gas}\right)}{R \times T}\right] = \gamma_j^{s,\infty} \times p_j^P \tag{28}$$

where, H_j^s, $\mu_j^{s,\infty}$, μ_j^{gas}, $\gamma_j^{s,\infty}$ and p_j^P are henry's law coefficient of compound 'j' in solvent 's', ideal gas phase chemical potential, infinite dilution state chemical potential, activity coefficient at infinite dilution and pure compound vapor pressure, respectively. Furthermore, the Gibbs' free energy of solvation are also calculated which is essentially the numerator in Eq. (28) i.e. the difference between the chemical potentials. The solvation free energies yield the free energy change associated with the transfer of a molecule between ideal gas and solvent at a particular temperature and pressure. The results are being presented in Fig. 8 and Table 13 for all the systems under study. A lower Henry's law coefficient value indicates higher CO_2 solubility [31]. Conclusively, at lower temperature of 303.15 K and at higher concentration of 2.432 mol.kg^{-1} of TESA, (2.528 + 0.498) mol.kg^{-1} (TESA + AEP) and (2.528 + 0.499) mol.kg^{-1} (TESA+APA) yield the maximum CO_2 physical solubility. Conversely, it can also be added a review that at higher concentration of AEP/APA, the solvents are expected to provide less physical but more chemical solubility for CO_2 absorption. Further, the constant is yielding a much lower value with respect to APA than AEP attributing to the fact that APA is a better chemical solvent for the same. The blends under study demonstrate a competitive physisorption behaviour which is generally a contributive property through misfit in the intermolecular interactions, hydrogen bonding and van der Waals forces of attraction. Henry's law coefficient for CO_2 and N_2O is obtained in the order: aq. TESA> aq. (TESA + AEP) > aq. (TESA + APA) systems.

3.8. Estimation of aqueous dissociation constants (pKa) of AEP and APA

Along with zwitterion formation, protonation is one of the important reactions in primary, secondary and tertiary amines during CO_2 capture process [48,60,61]. The dissociations constant (*pKa*) is also related to the rate constants of amines with CO_2. Traditionally, titration based methods are used for the determination of such dissociation constants. However, such methods are cumbersome. Hence, a prior prediction method is preferred for such calculations. In the present work, *pKa* values of AEP and APA are estimated. Single conformers of both AEP and

Table 13
COSMO predicted Henry's constant (*H* / bar) and Gibbs' free energy of solvation (*ΔGs* / kcal/mol) in temperature range of (303.15–323.15) K*.

			T/K				*T*/K				*T*/K		
		aq. TESA /(mol.kg^{-1})	303.15	313.15	323.15	(TESA + AEP) /(mol.kg^{-1})	303.15	313.15	323.15	(TESA + APA) /(mol.kg^{-1})	303.15	313.15	323.15
CO_2	*H*	2.432	909.627	1022.876	1132.019	2.528 + 0.498	784.184	882.403	977.482	2.528 + 0.499	779.737	877.824	972.864
	ΔG_s		4.104	4.313	4.516		4.015	4.221	4.421		4.011	4.218	4.418
N_2O	*H*		783.370	893.349	1000.729		675.798	770.921	864.151		668.549	763.153	855.996
	ΔG_s		4.014	4.228	4.436		3.925	4.137	4.342		3.919	4.130	4.336
CO_2	*H*	1.506	1384.119	1556.323	1720.963	2.259 + 0.756	820.271	922.923	1022.201	2.259 + 0.753	813.891	916.427	1015.735
	ΔG_s		4.357	4.574	4.785		4.042	4.249	4.450		4.037	4.244	4.446
N_2O	*H*		1155.215	1320.473	1481.238		701.080	800.049	897.035		690.275	788.510	884.969
	ΔG_s		4.248	4.472	4.688		3.947	4.160	4.366		3.938	4.151	4.357
CO_2	*H*	0.797	2064.195	2325.112	2573.800	2.044 + 1.004	842.927	948.405	1050.372	2.044 + 0.991	836.085	941.632	1043.856
	ΔG_s		4.598	4.824	5.043		4.058	4.266	4.467		4.054	4.261	4.463
N_2O	*H*		1666.567	1913.427	2153.983		715.467	816.750	916.024		702.488	802.998	901.772
	ΔG_s		4.469	4.702	4.929		−0.150	−0.089	−0.034		3.949	4.162	4.370

* 1 bar of gas per 1 mol of solvent is taken as reference state for *H* and *ΔGs* calculation.

APA were selected from the COSMO database. The corresponding cations of AEP and APA were formed in the 3D editor section of COSMOtherm using the initial geometry of the conformers present. Subsequently, the energies associated with each cation is calculated using Turbomole software. COSMOtherm computes the *pKa* values of any compound in a solvent based on the free energy change in the compound and corresponding cation of the compound in the solvent. Table 14 represents the *pKa* values of AEP and APA in various solvents at atmospheric temperature. The results indicate *pKa* value of APA are comparatively higher in comparison to AEP in all solvents indicating it to have better CO_2 solubility.

4. Conclusions

Concisely, thermodynamic analysis of potential blends of amines activators and reversible ionic liquid (TESA) which can be applied for the CO_2 capture process is presented. The study is carried out using COSMOtherm software. Suitability studies of selected solvents i.e. AEP, APA and TESA and their blends is done using sigma potential and sigma surface analysis. The results indicate that activator APA has better CO_2 selectively compared to TESA and AEP. In addition, aqueous blend of TESA and APA being a preferred solvent. Vapor pressures of the solvents, pure component density and viscosity are also simulated and compared with experimental data indicating a quality estimation through engaged technique. The maximum deviations for estimation of vapor pressure, density and viscosity in terms of % AAD are 6.922, 1.142 and 141.6, respectively. The Antoine equation coefficients relating the vapor pressure with temperature and concentration are also estimated. Inclusive of estimation of infinite dilution activity coefficients of the said systems reveal a highly non-ideal behaviour and subsequent deviations of the properties from ideality. Furthermore, activity coefficients based thermodynamic models viz. NRTL, WILSON and UNIQUAC 4 model binary interaction parameters are estimated for aq. (TESA), aq. (TESA + AEP), aq. (TESA + APA), and aq. (TESA + CO_2) systems. The results of vapor liquid equilibrium of the studies systems through the behaviour of activity coefficient, excess enthalpy, excess Gibbs' free energy and chemical potential indicate the highly non-ideal behaviour of all systems. CO_2 solubility in all the solvents are measured from (1.0–3.0) bar and (303.15–323.15) K. Additionally, predicted *pKa* values of AEP and APA indicate APA to have higher *pKa* values comparatively. This leads to the conclusion that APA reacts better to CO_2 when compared to AEP.

CRediT authorship contribution statement

Sweta Balchandani: Methodology, Investigation, Validation, Software, Writing - original draft. **Ramesh Singh:** Supervision, Conceptualization, Writing - review & editing.

Declaration of Competing Interest

The authors declare no competing financial interest.

References

[1] W. Bottinger, M. Maiwald, H. Hasse, Online NMR spectroscopic study of species distribution in MEA-H_2O-CO_2 and DEA-H_2O-CO_2, Fluid Phase Equilib. 263 (2008) 131–143.
[2] J.K. Carson, K.N. Marsh, A.E. Mather, Enthalpy of solution of carbon dioxide in (water + monoethanolamine, or diethanolamine, or n-methyldiethanolamine) and (water + monoethanolamine + N-methyldiethanolamine) at T=298.15 K, J. Chem. Thermodyn. 32 (2000) 1285–1296.
[3] A.M. Pinto, H. Rodriguez, A. Arce, A. Soto, Carbon dioxide absorption in the ionic liquid 1-ethylpyridinium ethyl sulfate and in its mixtures with another ionic liquid, Int. J. Greenh. Gas Cont. 18 (2013) 296–304.
[4] B.K. Mondal, S.S. Bandyopadhyay, A.N. Samanta, Equilibrium solubility measurement and kent-eisenberg modeling of CO_2 absorption in aqueous mixture of *N*-methyldiethanolamine and hexamethylenediamine, Greenh. Gases Sci. Technol. (2016) 1–13.
[5] A. Haghtalab, A. Shojaeian, High pressure measurement and thermodynamic modelling of the solubility of carbon dioxide in N-methyldiethanolamine and 1-butyl-3-methylimidazolium acetate mixture, J. Chem. Thermodyn. 81 (2015) 237–244.
[6] M. Mirarab, M. Sharifi, M.A. Ghayyem, F. Mirarab, Prediction of solubility of CO_2 in ethanol-[EMIM] [Tf_2N] ionic liquid mixtures using artificial neural networks based on genetic algorithm, Fluid Phase Equilib. 371 (2014) 6–14.
[7] A. Dey, S.K. Dash, S.C. Balchandani, B.P. Mandal, Investigation on the inclusion of 1-(2-aminoethyl) piperazine as a promoter on the equilibrium CO_2 solubility of aqueous 2-amino-2-methyl-1-propanol, J. Mol. Liq. 289 (2019) 111036.
[8] M. Safamirzaei, H. Modarress, Correlating and predicting low pressure solubility of gases in [bmim] [BF_4] by neural network molecular modelling, Thermochim. Acta 545 (2012) 125–130.
[9] J.S. Torrecilla, J. Palomar, J. Garcia, E. Rojo, F. Rodriguez, Modelling of carbon dioxide solubility in ionic liquids at sub and supercritical conditions by neural networks and mathematical regressions, Chemom. Intell. Lab. Syst. 93 (2008) 149–159.
[10] M.T. Mota Martinez, M.C. Kroon, C.J. Peters, Modeling CO_2 solubility in an ionic liquid: a comparison between a cubic and a group contribution EoS, J. Supercrit. Fluids 101 (2015) 54–62.
[11] X. Yang, R.J. Rees, W. Conway, G. Puxty, Q. Yang, D.A. Winkler, Computational modeling and simulation of CO_2 capture by aqueous amines, Chem. Rev. 117 (2017) 9524–9593.
[12] X. Wang, J. Chen, J. Mi, Structure-solubility correlation model for carbon dioxide in ionic liquids, Ind. Eng. Chem. Res. 52 (2013) 954–962.
[13] X.Y. Luo, F. Ding, W.J. Lin, Y.Q. Qi, H.R. Li, C.M. Wang, Efficient and energy saving CO_2 capture through the entropic effect induced by the intermolecular hydrogen bonding in anion-functionalized ionic liquids, J. Phys. Chem. Lett. 5 (2014) 381–386.
[14] J.C.L.Y. Fong, C.J. Anderson, G. Xiao, P.A. Webley, A.F.A. Hoadley, Multi-objective optimization of a hybrid vacuum swing adsorption and low temperature post combustion CO_2 capture, J. Clean. Prod. 111 (2016) 193–203.
[15] A. Nalaparaju, M. Khurana, S. Farooq, I.A. Karimi, J.W. Jiang, CO_2 capture in cation exchanged metal organic frameworks: holistic modeling from molecular simulation to process optimization, Chem. Eng. Sci. 124 (2015) 70–78.
[16] A. Mehrkesh, A.T. Karunanithi, Optimal design of ionic liquids for thermal energy storage, Comput. Chem. Eng. 93 (2016) 402–412.
[17] D. Moreno, V.R. Ferro, J.D. Riva, R. Santiago, C. Moya, M. Larriba, J. Palomar, Absorption refrigeration cycles based on ionic liquids: refrigerant/absorbent selection by thermodynamic and process analysis, Appl. Energy 213 (2018) 179–194.
[18] M.Z.M. Salleh, M.K. Hadj-Kali, M.A. Hashim, S. Mulyono, Ionic liquids for the separation of benzene and cyclohexane-COSMO-RS screening and experimental validation, J. Mol. Liq. 266 (2018) 51–61.
[19] D. Lazidou, S. Mastrogeorgopoulos, C. Panayiotou, Thermodynamic characterization of ionic liquids, J. Mol. Liq. 277 (2019) 10–21.
[20] X. Zhang, J. Pan, L. Wang, T. Qian, Y. Zhu, H. Sun, J. Gao, H. Chen, Y. Gao, C. Liu, COSMO-based solvent selection and Aspen plus simulation for tar absorptive removal, Appl. Energy 251 (2019) 113314.
[21] S. Huang, Z. Wang, S. Liu, R. Zhu, Z. Lei, Measurement and prediction of vapor pressure in binary systems containing the ionic liquid [EMIM] [DCA], J. Mol. Liq. 309 (2020) 113126.
[22] M. Fermeglia, S. Pricl, Multiscale molecular modeling in nanostructured material design and process system engineering, Comput. Chem. Eng. 33 (2009) 1701–1710.
[23] K. Mcbride, N.M. Kaiser, K. Sundmacher, Integrated reaction-extraction process for the hydroformylation of long-chain alkenes with a homogeneous catalyst, Comput. Chem. Eng. 105 (2017) 212–223.
[24] J. Esteban, M.G. Miquel, Thermodynamic insights on the viscometric and volumetric properties of binary mixtures of ketals and polyols, J. Mol. Liq. 263 (2018) 125–138.
[25] Z. Rashid, C.D. Wilfred, N. Gnansundaram, A. Arunagiri, T. Murugesan, Screening of ionic liquids as green oilfield solvents for the potential removal of asphaltene from simulated oil: COSMO-RS model approach, J. Mol. Liq. 255 (2018) 492–503.
[26] O. Alioui, Y. Benguerba, I.M. Alnashef, Investigation of the CO_2-solubiltiy in deep eutectic solvents using COSMO-RS and molecular dynamics methods, J. Mol. Liq. 307 (2020) 113005.
[27] V. Venkatraman, B.K. Alsberg, Predicting CO_2 capture of ionic liquids using machine learning, J. CO2 Utilization 21 (2017) 162–168.
[28] S. Balchandani, B.P. Mandal, S. Dharaskar, Measurements and modeling of vapor liquid equilibrium of CO_2 in amine activated imidazolium ionic liquid solvents, Fluid Phase Equilib. 521 (2020) 112643.
[29] A. Dey, B.P. Mandal, S.K. Dash, Analysis of equilibrium CO_2 solubility in aqueous APDA and its potential blends with AMP / MDEA for post combustion CO_2 capture, Int. J. Energy Res. (2020) https://doi.org/10.1002/er.5404.
[30] V. Blasucci, R. Hart, V.L. Mestre, D.J. Hahne, M. Burlager, H. Huttenhower, B.J.R. Thio, P. Pollet, C.L. Liotta, C.A. Eckert, Single component, reversible ionic liquids for energy applications, Fuel 89 (2010) 1315–1319.
[31] M.G. Miquel, M. Talreja, A.L. Ethier, K. Flack, J.R. Switzer, E.J. Biddinger, P. Pollet, J. Palomar, F. Rodriguez, C.A. Eckert, C.L. Liotta, COSMO-RS studies: structure-property relationships for CO_2 capture by reversible ionic liquids, Ind. Eng. Chem. Res. 51 (2012) 16066–16073.
[32] C.A. Eckert, C.L. Liotta, Reversible Ionic Liquids as Double-Action Solvents for Efficient CO_2 Capture, (technical report) Georgia Tech Research Corporation, Atlanta, 2011.
[33] F. Eckert, A. Klamt, COSMOtherm, Release 19.0.1, COSMOlogic GmbH & Co. KG, Leverkusen, Germany, 2013.
[34] K.Z. Sumon, A. Henni, Ionic liquids for CO_2 capture using COSMO-RS: effect of structure, properties and molecular interactions on solubility and selectivity, Fluid Phase Equilib. 310 (2011) 39–55.

[35] A. Klamt, F. Eckert, COSMO-RS: a novel and efficient method for the priori prediction of thermophysical data of liquids, Fluid Phase Equilib. 172 (2000) 43–72.
[36] P. Matheswaran, C.D. Wilfred, K.A. Kurnia, A. Ramli, Overview of activity coefficient of thiophene at infinite dilution in ionic liquids and their modeling using COSMO-RS, Ind. Eng. Chem. Res. 55 (2016) 788–797.
[37] S.K. Dash, A. Samanta, A.N. Samanta, S.S. Bandyopadhyay, Vapour liquid equilibria of carbon dioxide in dilute and concentrated aqueous solutions of piperazine at low to high pressure, Fluid Phase Equilib. 300 (2011) 145–154.
[38] R. Borgohain, B.P. Mandal, Thermally stable and moisture responsive carboxymethyl chitosan/dendrimer/hydrotalcite membrane for CO_2 separation, J. Membr. Sci. 608 (2020) 118214.
[39] A. Mondol, M. Barooah, B.P. Mandal, Effect of single and blended amine carriers on CO_2 separation from CO_2/N_2 mixtures using cross-linked thin-film poly (vinyl alcohol) composite membrane, Int. J. Greenh. Gas Cont. 39 (2015) 27–38.
[40] J. Hekayati, A. Roosta, J. Javanmardi, On the prediction of the vapor pressure of ionic liquids based on the principle of corresponding states, J. Mol. Liq. 225 (2017) 118–126.
[41] J.O. Valderrama, L.A. Forero, An analytical expression for the vapor pressure of ionic liquids based on an equation of state, Fluid Phase Equilib. 317 (2012) 77–83.
[42] D.Y. Peng, D.B. Robinson, A new two-constant equation of state, Ind. Eng. Chem. Fundam. 15 (1976) 59–64.
[43] A. Ahmady, A. Shamiri, M.A. Hashim, M.K. Aroua, Vapor pressure of aqueous methyldiethanolamine mixed with ionic liquids, J. Taiwan Inst. Chem. Eng. 45 (2014) 380–386.
[44] Z. Lei, G. Yu, Y. Su, C. Dai, Vapor pressure measurements and predictions for the binary and ternary systems containing ionic liquid [EMIM] [Tf_2N], J. Mol. Liq. 231 (2017) 272–280.
[45] M.H. Joshipura, S.P. Dabke, N. Subrahmanyam, Development and comparison of cohesion function relationship for PR equation of state, Int. J. Chem. Eng. Res. 1 (2009) 123–134.
[46] S. Kumar, H.C.M. Jae, Ionic liquid-amine blends and CO_2 BOLs: prospective solvents for natural gas sweetening and CO_2 capture technology-a review, Int. J. Greenh. Gas Cont. 20 (2014) 87–116.
[47] D. Wappel, G. Gronald, R. Kalb, J. Draxler, Ionic liquids for post-combustion CO_2 absorption, Int. J. Greenh. Gas Con. 4 (2010) 486–494.
[48] S. Paul, A.K. Ghoshal, B.P. Mandal, Kinetics of absorption of carbon dioxide into aqueous blends of 2-(1-piperazinyl)-ethylamine and *N*-methyldiethanolamine, Chem. Eng. Sci. 64 (7) (2009) 1618–1622.
[49] J.E. Bara, J.D. Moon, K.R. Reclusado, J.W. Whitley, COSMOtherm as a tool for estimating the thermophysical properties of alkylimidazoles as solvents for CO_2 separations, Ind. Eng. Chem. Res. 52 (2013) 5498–5506.
[50] M. Diedenhofen, F. Eckert, A. Klamt, Prediction of infinite dilution activity coefficients of organic compounds in ionic liquids using COSMO-RS, J. Chem. Eng. Data 48 (2003) 475–479.
[51] R. Putnam, R. Taylor, A. Klamt, F. Eckert, M. Schiller, Prediction of infinite dilution activity coefficients using COSMO-RS, Ind. Eng. Chem. Res. 42 (2003) 3635–3641.
[52] K. Paduszynski, An overview of performance of COSMO-RS approach in predicting activity coefficients of molecular solutes in ionic liquids and derived properties at infinite dilution, Phys. Chem. Chem. Phys. 19 (2017) 11835–11850.
[53] E.C. Voutsas, D.P. Tassios, Prediction of infinite-dilution activity coefficients in binary mixtures with UNIFAC, A Critical Evaluation. Industrial Engineering Chemistry Research, 35, 1996, pp. 1438–1445.
[54] S.K. Dash, A.N. Samanta, S.S. Bandyopadhyay, Solubility of carbon dioxide in aqueous solution of 2-amino-2-methyl-1-propanol and piperazine, Fluid Phase Equilib. 307 (2011) 166–174.
[55] H. Renon, J.M. Prausnitz, Local compositions in thermodynamic excess functions for liquid mixtures, Am. Inst. Chem. Eng. J. 14 (1968) 135–144.
[56] Y. Liang, H. Liu, W. Rongwong, Z. Liang, R. Idem, P. Tontowachwuthikul, Solubility, absorption heat and mass transfer studies of CO_2 absorption into aqueous solution of 1-dimethylamino-2-propanol, Fuel 144 (2015) 121–129.
[57] H. Ling, S. Liu, H. Gao, H. Zhang, Z. Liang, Solubility of N_2O, equilibrium solubility, mass transfer study and modeling of CO_2 absorption into aqueous monoethanolamine (MEA)/1-dimethylamino-2-propanol (1DMA2P) solution for post-combustion CO_2 capture, Sep. Purif. Technol. 232 (2020) 115957.
[59] T.J. Edwards, G. Maurer, J. Newman, J.M. Prausnitz, Vapor-liquid equilibria in multicomponent aqueous solutions of volatile weal electrolytes, AICHE J. 24 (6) (1978) 966–976.
[60] M. Afkhamipour, M. Mofarahi, A. Rezaei, R. Mahmoodi, C.H. Lee, Experimental and theoretical investigation of equilibrium absorption performance of CO_2 using a mixed 1-dimethylamino-2-propanol (1DMA2P) and monoethanolamine (MEA) solution, Fuel 256 (2019) https://doi.org/10.1016/j.fuel.2019.115877.
[61] A. Benamor, M.K. Aroua, Modeling of CO_2 solubility and carbamate concentration in DEA, MDEA and their mixtures using Deshmukh-Mather model, Fluid Phase Equilibria, 231, 2005, pp. 150–162.